Available online at www.sciencedirect.com

SciVerse ScienceDirect

Procedia Engineering 55 (2013) 457 – 462

Procedia Engineering

www.elsevier.com/locate/procedia

6th International Conference on Creep, Fatigue and Creep-Fatigue Interaction [CF-6]

Low Cycle Fatigue Damage of Mod.9Cr-1Mo Steel under Non-proportional Multiaxial Loading

Takamoto Itoh [a*], Kenichi Fukumoto [b], Hideki Hagi [c], Akira Itoh [a], Daichi Saitoh [a]

[a]University of Fukui, 9-1, Bunkyo 3-chome, Fukui-shi, Fukui 910-8507, Japan
[b]The Research Institute of Nuclear Engineering, University of Fukui, 1-2-4, Tsuruga-shi, 914-0055, Japan
[c]Fukui University of Technology, 6-5, Gakuen 3-chome, Fukui-shi, Fukui 910-8505, Japan

Abstract

This study discusses multiaxial low cycle fatigue damage of Mod.9Cr-1Mo steel under proportional and non-proportional loadings at room and high (823K) temperatures. Strain-controlled multiaxial low cycle fatigue tests were carried out using a hollow cylinder specimen including interruption tests. Strain paths employed were a push-pull straining, a reversed torsion straining and a circle straining. Behaviors of cyclic deformations and failure lives and an evaluation of the failure life are discussed. Surface cracks and microstructures in fatigued specimens are also observed by a digital microscope and a transmission electron microscope (TEM) in order to investigate mechanisms of cyclic deformation, failure and reduction in failure life due to non-proportional loading.

Keywords: Low cycle fatigue; multiaxial loading; mod.9Cr-1Mo steel; non-proportional loading; life evaluation

1. Introduction

Components and structures like pressure vessels and heat exchangers often undergo multiaxial low cycle fatigue (LCF) damage. In the multiaxial LCF under non-proportional loading in which directions of principal stress and strain change in a cycle, it has been reported that obvious life reduction has been observed depending on both strain path and material [1-8]. Deformation and life behaviors have been discussed and life evaluations have been proposed for various materials [2-7,9-13], but no study on high chromium steel, such as Mod.9Cr-1Mo steel employed in a first breeder reactor (FBR), has been reported. Development of an appropriate design parameter for multiaxial LCF for the reliable design and maintenance of structural components in FBR should be required.

In this study, strain-controlled multiaxial LCF tests of Mod.9Cr-1Mo by using a hollow cylinder specimen were performed under non-proportional loadings at room temperature and 823K. After the LCF tests,

* Corresponding author
E-mail address: itoh@u-fukui.ac.jp

doi:10.1016/j.proeng.2013.03.280

observations of crack by the digital microscope and microstructure by the TEM are also conducted. Based on the obtained results, the deformation and failure behaviors and life evaluation are discussed.

2. Material and experimental procedure

Material tested was a ferritic heat resisting steel, Mod.9Cr-1Mo steel. The specimen employed was the hollow cylinder specimen and the shape and dimensions of the specimen are shown in Fig. 1.

Strain-controlled multiaxial low cycle fatigue tests under non-proportional loadings were carried out at room temperature and 823K. In the test at 823K, the specimen was heated by a high frequency induction heater. The strain paths employed are three types as shown in Fig. 2, they are the push-pull straining (Push-pull), the reversed pure torsion straining (Rev. torsion) and the circle straining (Circle). Push-pull and Rev. torsion tests are the proportional strain loading tests and Circle test is the non-proportional strain loading test in which axial strain (ε) and shear strain (γ) have 90° phase difference. Total axial strain and total shear strain ranges ($\Delta\varepsilon$ and $\Delta\gamma/\sqrt{3}$) were the same ranges based on von Mises. Strain rate was 0.1%/sec based on von Mises basis. Number of cycles to failure (failure life), N_f, is determined as the cycles at which axial or shear stress range was reduced to 3/4 from that at $1/2N_f$.

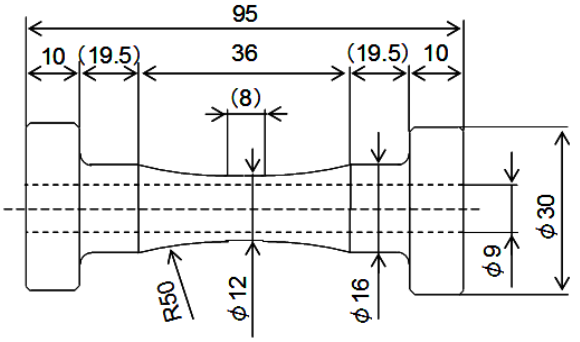

Fig. 1. Shape and dimensions of specimen (mm).

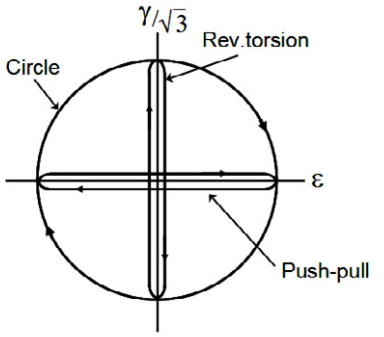

Fig. 2. Strain paths employed.

Interruption tests were also carried out in order to take observations of crack by the digital microscope and microstructure by TEM.

3. Experimental results and discussion

3.1. Failure life and life evaluation

Figure 3 shows failure lives (N_f) correlated by an equivalent total strain range based on Mises. In the figure, the bold dashed and solid lines are drawn based on the data of Push-pull test and the two thin dashed and solid lines show a factor of 2 band at room temperature and 823K, respectively. In the test at room temperature, although only the two data are plotted, the reduction in failure life due to non-proportional loading can be seen. N_f in Circle test is correlated out of the band. At 823K, N_f in Circle tests are overestimated as well as that at room temperature although the reduction ratio of life due to non-proportional loading seems to be smaller in higher strain level. N_f in Rev. torsion test are almost the same as those in Push-pull test.

Itoh *et al.* [2,4-6,8] proposed a non-proportional strain range as a strain parameter for life evaluation under non-proportional loading equated as,

$$\Delta\varepsilon_{NP} = (1 + \alpha f_{NP})\Delta\varepsilon_I \qquad (1)$$

where $\Delta\varepsilon_1$ is the maximum principal strain range under non-proportional loading which can be calculated by ε and γ [8,14]. α and f_{NP} are the material constant and non-proportional factor, respectively. The former is the parameter related to the additional hardening due to non-proportional loading and the latter is the parameter expressing the intensity of non-proportional loading.

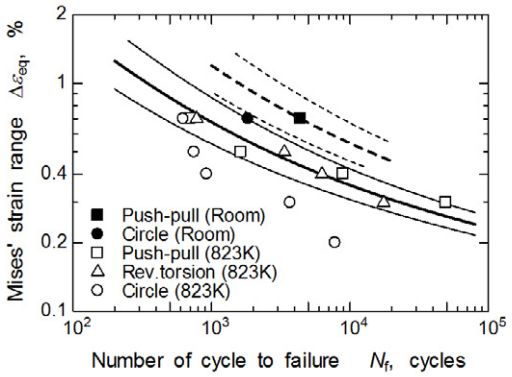

Fig. 3. Correlation of failure life by $\Delta\varepsilon_{eq}$.

The value of α is defined as the ratio of increase in stress amplitude in Circle test to that in Push-pull test. f_{NP} is defined by integral equation measuring the rotation of the maximum principal strain direction and the integration of strain amplitude after the rotation. Therefore, f_{NP} totally evaluates the severity of non-proportional loading in a cycle. f_{NP}=0 in Push-pull and Rev. torsion tests for proportional loading paths, f_{NP}=0–1 in non-proportional loading paths and f_{NP}=1 in Circle test.

Figure 4 shows a comparison of cyclic stress-strain curves in Push-pull and Circle tests for Mod.9Cr-1Mo obtained in step-up tests. This figure clearly shows that there is no additional hardening due to non-proportional loading. Thus, if the value of α is evaluated as mentioned above, α takes 0. However, Mod.9Cr-1Mo had the significant reduction in failure life due to non-proportional loading as shown in Fig. 3. Consequently, α was evaluated by a simple equation proposed by Itoh [8] and equated as,

$$\alpha = \mathrm{S}\,\frac{(\sigma_B - \sigma_Y)}{\sigma_B} \qquad (2)$$

where σ_B is tensile strength and σ_Y yielding or 0.2% proof stress. The coefficient S takes S=1 for FCC materials and S=2 for BCC materials. The value of α obtained by Eq. (2) was α=0.5 for Mod.9Cr-1Mo at both room temperature and 823K. Figure 5 shows N_f correlated by $\Delta\varepsilon_{NP}$ with α=0.5. All the data can be correlated within the factor of 2.

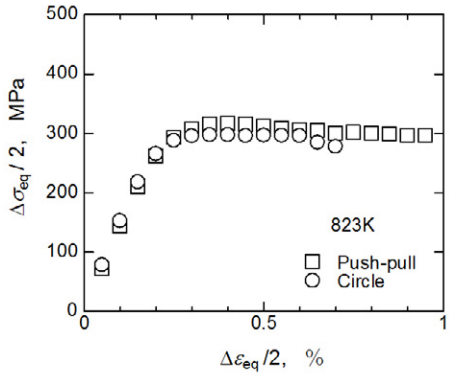

Fig. 4. Cyclic stress-strain curve.

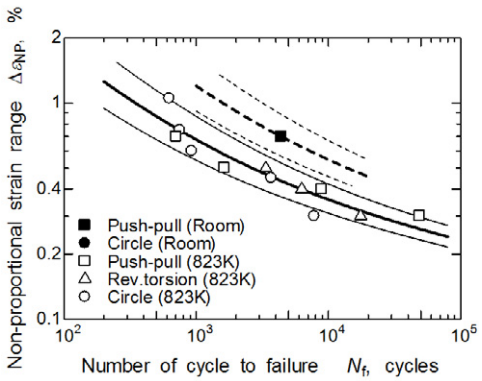

Fig. 5. Correlation of failure life by $\Delta\varepsilon_{NP}$ (α=0.5).

3.2. Cyclic deformation property

Figure 6 shows stress amplitude as a function of number of cycle in Push-pull and Circle tests. In the figure, stress amplitudes are normalized by the maximum stress amplitude ($\sigma_{eq}/\sigma_{max\ eq}$) and the number of cycle by failure cycle (N/N_f). In all the tests, cyclic softening can be seen and $\sigma_{eq}/\sigma_{max\ eq}$ becomes constant values at room temperature except final cycles and decreases continuously at 823K. The degree of reduction in $\sigma_{eq}/\sigma_{maxeq}$ with increasing cycle by N/N_f=0.2 at both room temperature and 823K in Circle test takes larger than those in Push-pull test.

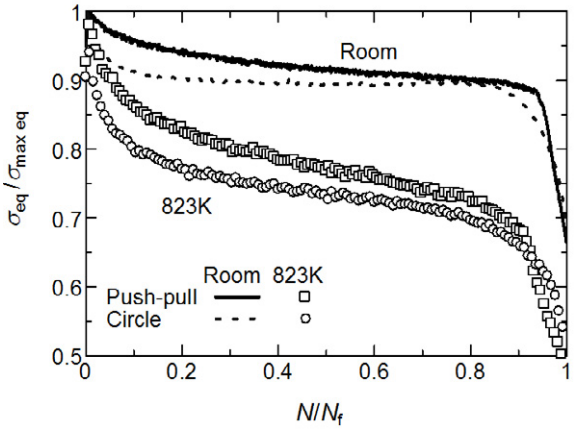

Fig. 6. Variation of stress ratio *vs* life ratio.

Degree and rate of cyclic softening until N/N_f=0.2 in the Circle test are larger than those in the Push-pull test, which may be related to creation of sub-grain easily under non-proportional loading.

3.3. Crack and microstructure

Figure 7 shows surface crack and microstructure observed in the interruption tests at room temperature. In Push-pull test, no crack is observed during N/N_f=0.1−0.5. A main crack is observed normal to axial direction and small cracks also observed near by the main crack at N/N_f=1. In Circle test, no crack was observed during N/N_f=0.1−0.3 but surface of specimen was roughed at N/N_f=0.3. The roughness becomes more remarkable at N/N_f=0.5 but obvious small crack was not observed. At N/N_f=1, small cracks are observed and the number of the crack are much larger than that in Push-pull test. Crack behaviors in Push-pull and Circle tests at 823K are the similar to those at room temperature.

The main cracks observed normal to axial direction whose length is relative large are crated in Push-pull test and many small cracks are observed into various directions in Circle test. The latter may be caused by direction change of principal stress and strain in the circle strain path.

Microstructure at P2 in Push-pull test shows dislocation bundles in lath structure which is typically shown in martensitic structure and the initiation of sub-grain. At P3, more clear sub-grains are observed and the number of dislocations in the grain becomes much less, which is continued to P4. In Circle test, dislocation bundles can be seen in early cycle, at C1, and the microstructure takes ladder structure with the creation of sub-grains. The observation of the sub-grain becomes clearer with increasing the cycle to C3 and C4.

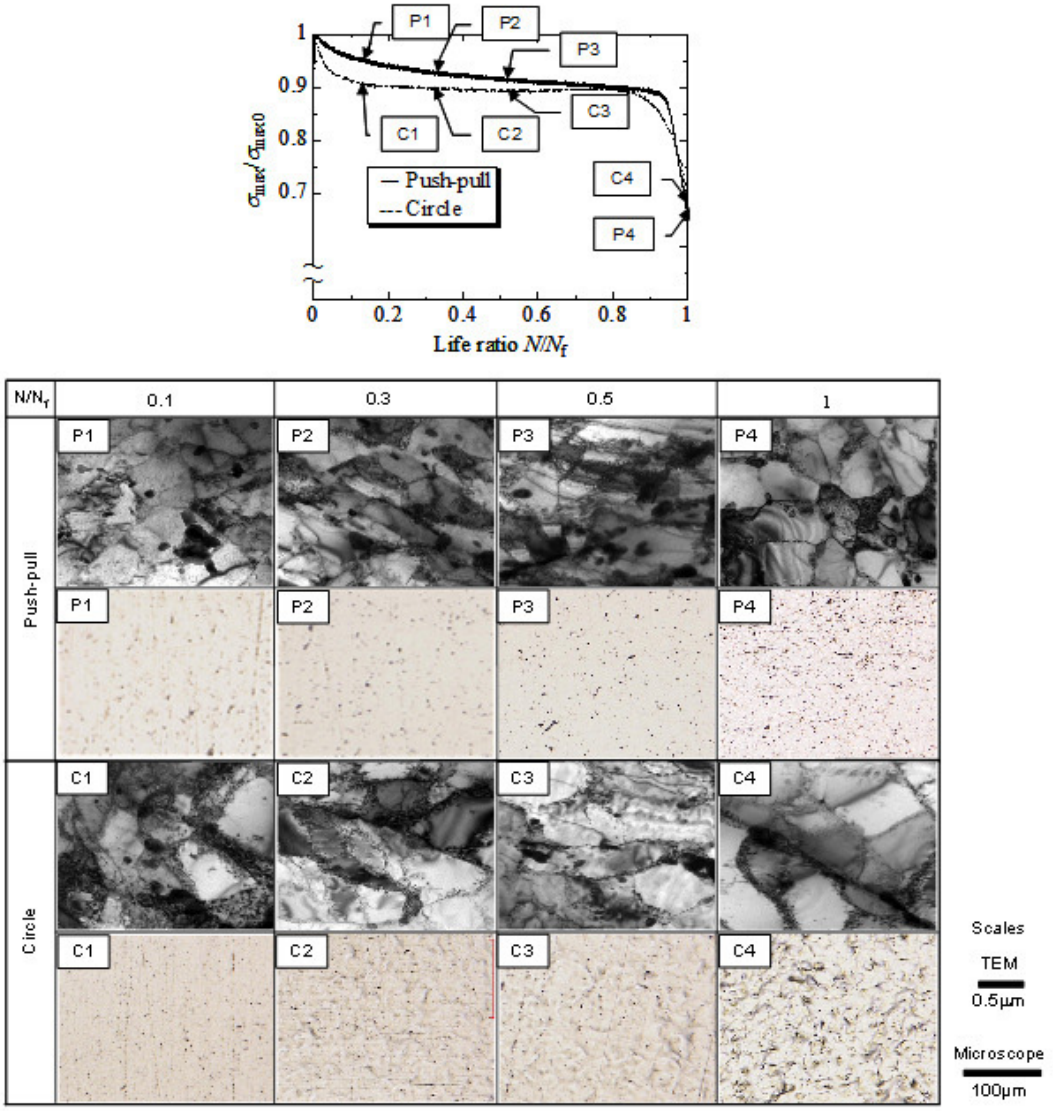

Fig. 7. TEM and surface crack observations at each life ratio in interrupted tests.

Figure 8 shows a relationship between averaged sub-grain size ($\overline{d}$) and life ratio (N/N_f). Properties of the increase in size of the sub-grain correspond well to the cyclic softening behaviors shown in Fig. 7. In the final stage, at N/N_f=0.8 and in later, the value of $\overline{d}$ in Push-pull test takes larger than that in Circle test. The results may came from that the initiation of many small cracks in Circle test contribute to open the crack easier resulting in the reducing the crack propagation rate due to smaller damage for each crack.

The above can be summarized as follows. The reduction in failure life due to non-proportional loading is caused by initiation of many small cracks in various directions. However, since the cycle of the initiation of the small cracks was later than the half of life, additional cyclic softening is not caused by the initiation of small cracks but by the increase in the size of sub-grains due to non-proportional loading.

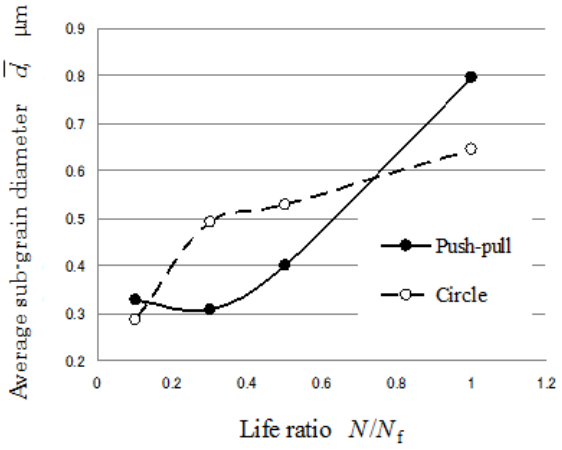

Fig. 8. Averaged sub-grain size *vs* life ratio.

4. Conclusions

1. Mod.9Cr-1Mo steel showed the drastic reduction in failure life but showed no additional hardening due to non-proportional loading at room and 823K.
2. The failure lives were evaluated well by the non-proportional strain range in which material constants were obtained by using the simple equation with monotonic tension test data, α=0.5.
3. Reduction in failure life due to non-proportional loading may be resulted from the creation of larger number of cracks oriented to various directions.
4. The additional cyclic softening due to non-proportional loading resulted from coarsening of sub-grain.

Acknowledgement

Present study includes the result of "Core R&D program for commercialization of the fast breeder reactor by utilizing Monju" entrusted to University of Fukui by the Ministry of Education, Culture, Sports, Science and Technology of Japan (MEXT).

Reference

[1] S.H.Doong, D.F.Socie, I.M.Robertson, *Trans. American Society of Mech. Engineers, J. Engg. Mater. Tech.*, 1990; 112: 456-464.
[2] T.Itoh, M.Sakane, M.Ohnami, K.Ameyama, *J. Soc. Mater. Sci., Japan*, 1992; 41: 1361-1367. (in Japanese).
[3] C.H.Wang, M.W.Brown, *Fatigue & Fracture of Engg. Mater. & Structures*, 1993; 16: 1285-1298.
[4] T.Itoh, M.Sakane, M.Ohnami, D.F.Socie, *Trans. American Society Mechanical Engineers, J. Engg. Mater. Tech.*, 1995; 117: 285-292.
[5] T.Itoh, M.Sakane, M.Ohnami, D.F.Socie, *Trans. American Soc. Mech. Engineers, J. Engg. Mater. Tech.*, 117(1995)285-292.
[6] T.Itoh, T.Nakata, M.Sakane, M.Ohnami. *European Structural Integrity Society*, 25(1999)41-54.
[7] D.F.Socie, G.B.Marquis, Multiaxial fatigue, *Society of Automotive Engineers International*, 2000, pp.129-339.
[8] T.Itoh, T.Yang, *Intl. J. Fatigue*, 33(2011)1025-1031.
[9] A.Nitta, T.Ogata, K.Kuwabara, *J. Society of Mater. Sci., Japan*, 36(1987)376-382. (in Japanese)
[10] S.H.Doong, D.F.Socie, *Trans. American Soc. Mech. Engineers, J. Engg. Mater. Tech.*, 113(1991)23-30.
[11] A.Carpinter, R.Brighenti, E.Macha, A.Spagnoli, *Intl. J. Fatigue*, 21(1999)89-96.
[12] L.Reis, B.Li, M.de Freitas, *Intl. J. Fatigue*, 31(2009)1660-1668.
[13] K.Tokimasa, S.Sagara, D.Fujinaka, *J. Soc. Mater. Sci., Japan*, 58(2009)143-148. (in Japanese).
[14] T.Itoh, M.Sakane, T.Ozaki, *J. Soc. Mater. Sci., Japan*, 60(2011)88-93. (in Japanese).